Proceedings of the XVII ECSMGE-2019
Geotechnical Engineering foundation of the future
ISBN 978-9935-9436-1-3

doi: 10.32075/17ECSMGE-2019-0400

XVII European Conference
ECSMGE 2019
Reykjavik
on Soil Mechanics
and Geotechnical Engineering

. A conceptual model to demonstrate the role of suction in the formation of head-cut in fine-grained embankments subjected to overflow

Un modèle conceptuel pour dèmontrerer le rôle de la suction dans la formation d'une head-cut dans des digues de sols fins soumis à un debordement

L. Adinolfi & A.Tarantino
University of Strathclyde, Glasgow, United Kingdom

ABSTRACT: Breaching induced by overflow is one of the most important causes of failure of flood defence embankments. In fine-grained embankments, breaching tends to develop from the toe towards the crest. This mechanism is referred to as 'head-cut erosion' and has been attributed mainly to hydrodynamic effects, i.e. higher flow velocity and turbulence at the downstream toe. However, this hydrodynamic condition also occurs in non-cohesive embankments where mechanisms of breaching are substantially different. In this study, we elucidate a second mechanism potentially contributing to the head-cut formation. The clay forming the embankment is exposed to the atmosphere and is generally in an unsaturated state at the onset of the overflow. The infiltration process associated with this condition is responsible of a loss of suction and, hence, of shear strength. This paper presents a very simple conceptual model aimed to demonstrate that the formation of the head-cut can be explained in terms of shear strength loss, which is higher at the toe of the embankment than at the crest. It is shown that simple 'erosion' can be interpreted as a succession of mini-slope instabilities associated with typical hydraulic and mechanical process occurring in slopes.

RÉSUMÉ: Les brèches causées par débordement sont l'une des principales causes de défaillance des digues de protection contre les inondations. Dans les remblais construits avec des sols argileux, la rupture a tendance à se développer de la base vers la crête. Ce mécanisme est appelé «head-cut erosion» et a été attribué principalement aux effets hydrodynamiques dus à la vitesse plus élevée de l'écoulement et à la turbulence au niveau de la base. Cependant, cette condition hydrodynamique se produit également pour les remblais non cohésifs où les mécanismes de rupture sont substantiellement différents. Il apparaît donc que les forces hydrodynamiques seules ne suffisent pas à expliquer la formation du «head-cut». L'argile formant le remblai est exposée à l'atmosphère et se trouve généralement à l'état insaturé au début du débordement. Le processus d'infiltration associé à cette condition est responsable d'une perte de succion et donc d'une perte de résistance au cisaillement. Cet article présente un modèle conceptuel très simple visant à démontrer que la formation de la coupe de tête peut être expliquée en termes de perte de résistance au cisaillement, qui est plus élevée au pied du remblai. Il est montré que la simple "érosion" peut être interprétée comme une succession d'instabilités de mini-pente associées à des processus hydrauliques et mécaniques typiques se produisant dans les pentes.

Keywords: embankment; overflow; head-cut; fine-grained geomaterials; suction

1 INTRODUCTION

Statistical studies of historical earthen embankment failures have shown that, overflow is the most common triggering mechanisms among other ones, i.e. piping, foundation, structural defects (Foster, Fell, & Spannagle, 2000; Wu, 2011).

Overflow may occur during extreme flood or because of settlements of the embankment crest. In these situations, water levels rise over the embankment crest inducing a gradual flow of water along the downstream slope. The hydrodynamic forces associated with the water flow tend to excavate a channel along the slope, which eventually evolves into the final breach. Extent and progression of the breach channel are dependent on the water flow, the nature and state of the filling materials (i.e. rock-fill, coarse-grained, fine-grained) and the type of structure (e.g. homogeneous, composite, presence of accessory structures, design and construction method) (Morris, 2009).

In the last decades, many researchers have been investigated the role of the construction materials. Large-scale physical tests (Hanson et al., 2005; Hassan and Morris, 2008; Walder, J. S., et al., 2015) and small-scale laboratory models on homogeneous prototypes (Morris et al., 2007; Zhao, 2016) showed that two main characteristic erosion behaviours differentiate breach initiation and growth in coarse-grained and fine-grained embankments respectively. Coarse-grained fills tend to erode quickly according to a progressive surface erosion mechanism, which flattens the face up to the crest, as result of tangential flow stresses (Figure 1a). Breaching of clay embankment is usually much slower and characterized by head-cut erosion, which consists of the formation of a stepped, non-uniform profile of the landward slope (Morris, 2009b, Volz, 2013, Wu, 2011) (Figure 1b). The small over falls observed initially tend to merge into a few or even a single larger head-cut that progressively propagates backwards (Morris, 2009a). The two erosion behaviours tend to assume the same characteristics once that the crest is reached, inducing a drastic change of the water flow with a sudden increase of the discharge.

This experimental evidence still needs to be fully explained and there are some key questions that have not yet been answered. In particular, (1) why there is a substantially different mode of failure between fine-grained and coarse-grained embankments and (2) why the failure process starts from the toe in fine-grained embankments.

Most of the studies undertaken so far tend to answer to the second question by assuming that near the downstream toe the hydrodynamic shear stresses exerted by the flow are the highest and therefore they are able to start removing material from the toe first. However, higher hydrodynamic shear stresses also occur in coarse-grained structures, but the process of breach formation observed is very different, the crest being the most vulnerable part. Hence, it seems that hydrodynamic forces alone are not sufficient alone to explain the head-cut formation.

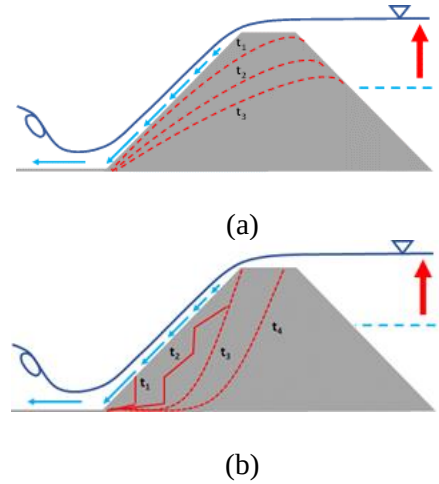

Figure 1. (a) Surface erosion in coarse-grained embankments and (b) Headcut erosion mechanism in fine-grained embankments.

Regarding the first question, Morris, 2011, explains for example that head-cut erosion is the predominant mechanism in fine-grained soils because by fine-grained soils are less erodible than

coarse-grained materials and are able to sustain the formation of steps.

However, recent experimental investigations, (Walder, J. S., R. M. Iverson, J. W. Godt, M. Logan, 2015, Pickert, Weitbrecht, & Bieberstein, 2011, Al-Riffai & Nistor, 2010) have shown that head-cut formation also occurs in coarse-grained embankment, where negative pore-water pressures exist.

Overall, there seems to be a relatively poor understanding of the mechanical and physical processes behind the concept of erodibility and breach formation.

The head-cut formation observed in coarse-grained embankment with initial negative pore-water pressures suggests that partial saturation and suction may play a key role in the response of the embankment to overflow. Indeed, the embankment is unsaturated at the onset of overflow and the infiltration process towards the core of the embankment induced by overflow may provide another possible explanation of the physical processes observed.

2 TOWARDS A NEW CONCEPTUAL MODEL FOR BREACH FORMATION

The fundamental idea that inspired the proposed conceptual model is based on the observation that the soil forming the embankment is usually in an unsaturated state at the onset of overflow.

Suction and the degree of saturation govern soil behaviour. It is well known that shear strength and stiffness in unsaturated soils are higher than saturated soils (Tarantino & El Mountassir, 2013).

The independent contribution of suction and degree of saturation ate highlighted by the ultimate shear strength equation for unsaturated soils (Tarantino & El Mountassir, 2013):

$$\tau = \sigma'' tg\varphi' = (\sigma + sS_r) tg\varphi' \qquad (1)$$

where σ'' (kPa) is the Bishop's effective stress, σ (kPa) is the total stress, s is suction (kPa), S_r is the degree of saturation and φ' is the 'saturated' angle of shearing resistance.

The additional term of the shear strength is fleeting, in the sense that it disappears once that suction drops to zero. However, the soil constituting the embankment can take advantage of this enhanced strength for relatively long time, since the unsaturated state tends to persist also during extreme flood events.

The initial increase of levels in the water body induces an inward water flow from the upstream zone (Figure 2a,b). At the onset of the overflow, the downstream zone is still unsaturated. Once the overflow establishes, the downstream slope experiences in turn a transient infiltration process (Figure 2c).

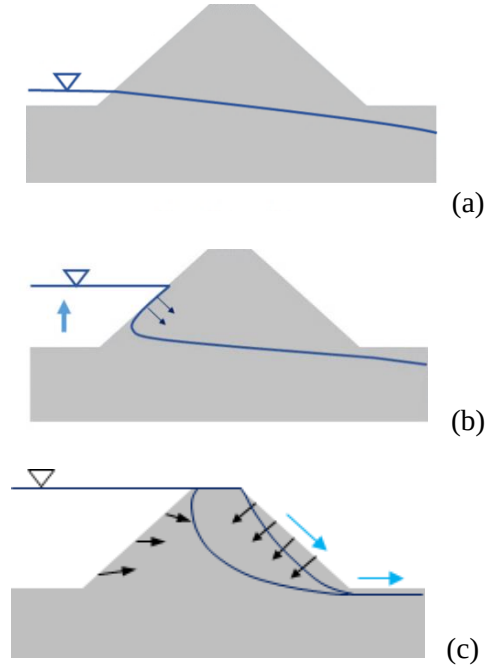

Figure 2. Water flow and propagation of the saturation front within an embankment during overflow (a) initial condition (b) increase in water level (c) overflow and infiltration

As the overflow proceeds fuelling the inward infiltration, the degree of saturation tends to increase and suction tends to decrease in the most superficial layers of the downstream slope. At a

certain point, the suction drops to zero, together with the additional shear strength related to the suction.

The part of the embankment more vulnerable in this scenario is the toe, being the point in which the two saturation fronts propagating from the upstream and downstream slopes respectively are likely to meet first. Therefore, the soil in the toe zone, close to a saturated state, experiences a faster reduction of the shear strength and for this reason is more prone to fail than soil in regions faraway.

A typical stress state near the toe and another one near the crest is represented in the Mohr plane, for the initial condition and the overflow phase (Figure 3). It is evident that the change of effective stress is more significant at the toe and it could lead to touch the failure envelope. This loss of strength might explain the reason why the onset of breaching has been observed at the toe.

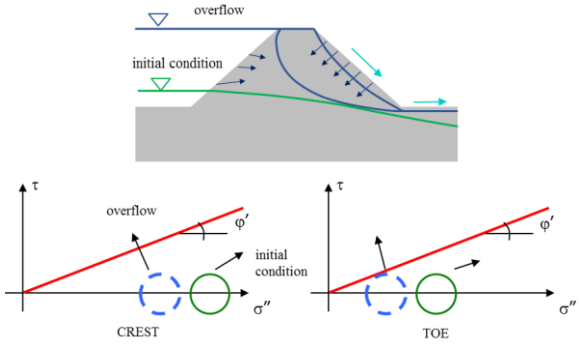

Figure 3. Change of effective stress along the downstream face

3 PROOF OF CONCEPT: THE INFINITE SLOPE CASE

A very simple approach is presented here to estimate the effects of the inward infiltration and the consequent loss of strength of the embankment material in the superficial layers of the downstream slope.

The downstream slope has been idealised as an unsaturated infinite slope to calculate the changes of the factor of safety during infiltration.

This requires the knowledge of the state of effective stresses within the slope, which varies continuously in space and time, according to the distribution of the pore-water pressures driven by the transient water flow.

3.1 Water Flow Analysis

The infiltration process related to the overflow is studied by adopting a simplified analysis. The water flow is assumed to take place in vertical direction and described by the following equation:

$$\frac{\partial}{\partial z}(v_z) = -\frac{\partial \theta}{\partial t} \tag{2}$$

where v_z *(m/s)* is the flow velocity in the vertical direction, θ is the volumetric water content (volume of water per total volume), and t is the time (s).

$$\frac{\partial \theta}{\partial t} = n\frac{\partial S_r}{\partial t} + S_r\frac{\partial n}{\partial t} \tag{3}$$

$$v_z = -k\frac{\partial h}{\partial z} = -k\frac{\partial}{\partial z}\left(\frac{u_w}{\gamma_w} + z\right) \tag{4}$$

where u_w is the pore-water pressure (kPa), z is the vertical coordinate (m), γ_w (kN/m^3) is the specific weight of water, and k is the hydraulic conductivity (m/s). Combining equations (2), (3) and (4):

$$\partial/\partial z\left[k(u_w)\ \frac{\partial}{\partial z}\left(\frac{u_w}{\gamma_w} + z\right)\right] = n\frac{\partial S_r}{\partial u_w}\frac{\partial u_w}{\partial t} \tag{5}$$

Two hypotheses have been adopted to simplify equation (5), (a) the hydraulic conductivity is assumed to be equal to the saturated value k_{sat} (maximum infiltration and hence maximum reduction of suction), and (b) linearization of the soil water retention curve (SWRC) such that

$$n\frac{\partial S_r}{\partial u_w} \sim n\frac{\Delta S_r}{\Delta u_w} = \frac{\Delta \theta}{\Delta u_w} = constant \tag{6}$$

and:

$$\left(\frac{k_{sat}}{\gamma_w \frac{\Delta\theta}{\Delta u_w}}\right)\frac{\partial u^2}{\partial z} = \frac{\partial u_w}{\partial t} \quad (7)$$

The term in parentheses is equivalent to the consolidation coefficient in the Terzaghi's consolidation equation for saturated soils

$$C_{v,unsat} = \frac{k_{sat}}{\gamma_w \frac{\Delta\theta}{\Delta u_w}} \quad (8)$$

The final equation is given as:

$$C_{v,unsat}\frac{\partial u^2}{\partial z} = \frac{\partial u_w}{\partial t} \quad (9)$$

Equation (9) is reduces to the Terzaghi's consolidation 1-D equation that can be solved analytically (Tarantino & El Mountassir, 2013).

3.2 *Factor of safety of an unsaturated infinite slope*

The factor of safety is calculated by considering the equilibrium of a slice of unitary width (Figure 3) and because of equation (1):

$$FS = \frac{\tau_{lim}}{\tau} = \frac{\sigma \cdot tg\varphi' + (-u_w)\cdot S_r \cdot tg\varphi'}{\tau} \quad (10)$$

$$FS = \frac{z\cdot\gamma\cdot cos^2\alpha\cdot tan\phi\prime}{\tau + z\cdot\gamma\cdot sin\alpha\cdot cos\alpha} + \frac{(-u_w)\cdot S_r\cdot tan\phi\prime}{\tau + z\cdot\gamma\cdot sin\alpha\cdot cos\alpha} \quad (11)$$

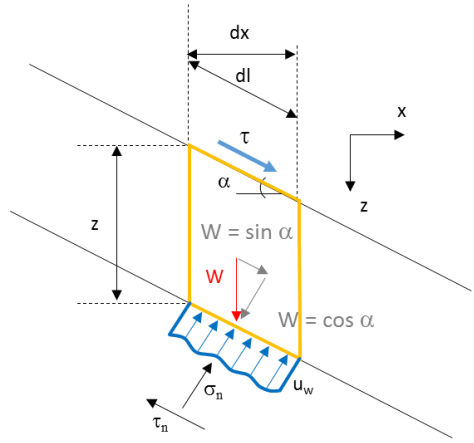

Figure 4. Forces acting in an infinite slope.

where γ_w (kN/m^3) is the specific weight of water, γ (kN/m^3) is the specific weight of the soil, z is the vertical coordinate (m), φ' is the soil friction angle (rad), u_w is the pore-water pressure (kPa) and S_r is the degree of saturation (-), τ is the hydraulic shear stress (kPa) exerted by the hydrodynamic flow.

3.3 *Application to an ideal case*

With reference to an ideal homogeneous embankment (Figure 5), the downstream slope has been divided into three strips P1, P2, P3. The hydraulic shear stresses have been evaluated via computational fluid dynamic (CFD) with the software OpenFoam, simulating an overflow process with a *k-ε* turbulence model.

The initial phreatic surface is assumed to horizontal and to pass through the toe of the embankment. The distribution of pore-water pressures with depth is therefore assumed to be initially hydrostatic.

Table 1. Embankment Geometry

Property	P1	P2	P3
Slope (°)	18	18	18
Distance from Water Level (m)	6	4	2
Hydraulic Shear Stress (kPa)	0.125	0.185	0.204

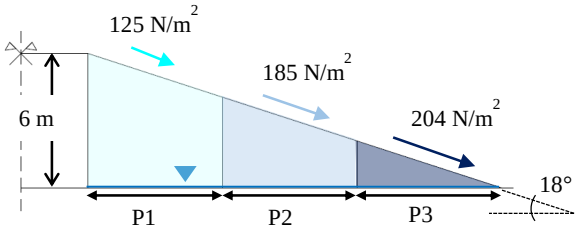

Figure 5. Slope geometry and divisions in three strips

For the three strips P1, P2, and P3, the values of suctions at the top of the strip are 60 kPa, 40 kPa, and 20 kPa respectively. The highest value of suction is 60 kPa on the crest of the embankment.

The soil water retention function and the hydraulic conductivity function considered in this exercise are shown in Figure 6 and 7 respectively. These represent a silty material.

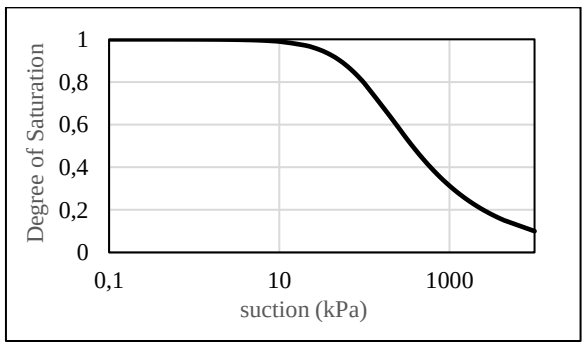

Figure 6. Soil Water Retention function

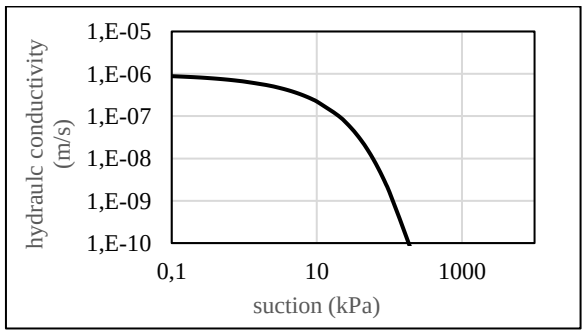

Figure 7. Hydraulic Conductivity function

The degree of saturation, the hydraulic conductivity, and the slope of the water retention curve at the top of each strips are determined from Figure 6 and Figure 7 respectively by considering the values of suction at the top of each strip. The slope $\frac{\Delta\theta}{\Delta u_w}$ is derived by considering the tangent to the water retention function at the value of suction at the top of the strip. The details of the material properties are presented in Table 2 for the three segments.

Table 2. Material Properties

Property	**P1**	**P2**	**P3**
φ'(°)	18	18	18
γ (kN/m^3)	19	19	19
s=-u_w (kPa)	60	40	20
k_{sat} (m/s)	10^{-9}	10^{-8}	10^{-7}
$\frac{\Delta\theta}{\Delta u_w}$	0.0008	0.0007	0.0005
$C_{v,unsat}$	1.25 E-07	1.43 E-06	2.00 E-05
S_r	0.88	0.93	0.97

4 RESULTS

Equation 9 was first solved to provide the evolution of pore-water pressure profile with time and Equaiton 11 was then used to calculate the Factor of Safety (FS) based on the pore-water pressure derived from Equation 9.

In the following, three different times of exposure to overflow have been considered: 1 hour, 5 hours and 24 hours. In addition, the Factor of Safety has been calculated with and without the presence of the hydrodynamic shear stresses, which develops at the interface soil-water because of the water flow.

The results are plotted Figure 8, 9 and 10 for the strips P1, P2, and P3 respectively. For the strip P1 (Figure 8), the FS on the crest is the highest and the effect of the hydraulic shear stress appears to be negligible. Here the hydraulic conductivity is very low due to the relatively high initial suction and FS profiles vary very little over time.

For the strip P2 (Figure 9), the FS reduces, more significantly and the effects of the hydrodynamic shear stresses become more important mainly in the first 50 cm and for the overflow time of 1 hour. On the other hand, when the suction drops considerably after 24 hours of overflow, the effects of the hydrodynamic shear stresses tend to reduce.

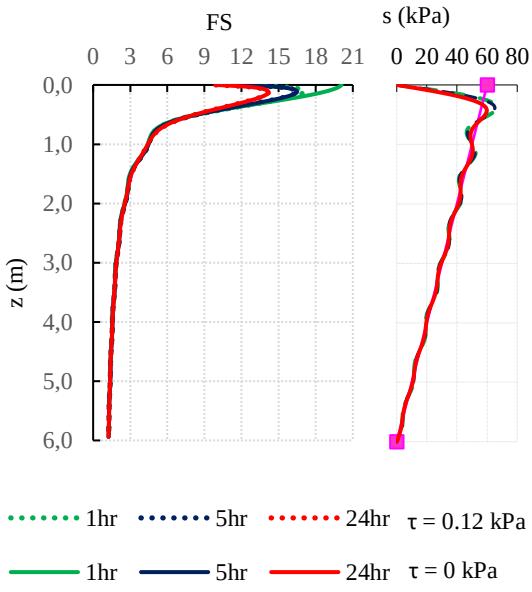

Figure 8. Factor of Safety and suction profile for P1 with and without hydraulic shear stresses for time of overflow 1 hr, 5 hr and 24 hr.

The strip P3 (Figure 10) shows the lowest value of the FS with FS becoming lower than unity when the presence of the hydrodynamic shear stresses are considered. This occurs at very shallow depth (4 cm for overflow of 1 hr and 5 hrs and 13 cm for overflow of 24 hrs).

The effect of hydraulic shear stresses is again more relevant for an overflow of 1 hr than for overflow of 5 hrs and 24 hrs.

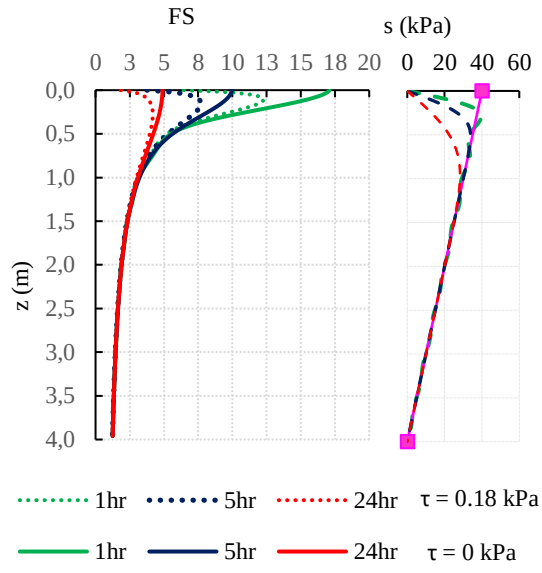

Figure 9. Factor of Safety and suction profile for P2 with and without hydraulic shear stresses for time of overflow 1 hr, 5 hr and 24 hr.

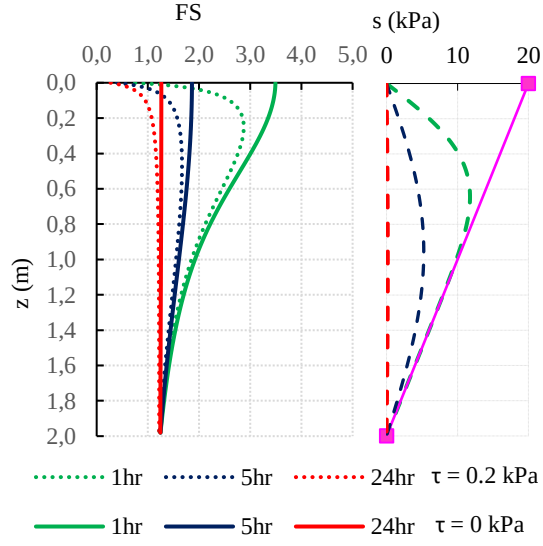

Figure 10. Factor of Safety and suction profile for P3 with and without hydraulic shear stresses for time of overflow 1 hr, 5 hr and 24 hr.

5 CONCLUSIONS

A conceptual model to study the effects of infiltration on the stability of the downstream slope of

earth embankment was presented. A simplified approach, based on 1-D water flow solution applied to an infinite slope was adopted. The simplified water flow equation was based on the linearization of the water retention curve and a constant value the hydraulic conductivity (equal to the saturated one). The factor of safety of the infinite slope was calculated considering the contribution of suction on soil strength.

The most important outcome is that the hydraulic conductivity of the material seems to govern the process. For very low value (i.e. $k = 10^{-9}$ m/s), which occurs on the highest part of the downstream slope, the FS does not change significantly with time. The high values of FS found here, show that the crest is the most stable part during an overflow, because the hydraulic shear stresses are small and the suction-induced apparent cohesion tends to be maintained.

In this exercise, the upper and middle part of the downstream slope remained stable, whereas the toe became unstable. This was due to the lower initial suction at the toe which generated a relatively high hydraulic conductivity and a more rapid loss in suction during overflow. In this exercise, first 4 cm were "washed away" (FS = 0.72). The destabilizing effects of the hydraulic shear stresses are predominant in the early stage of overflow, but their influence tends to decrease when a longer exposure is considered, which causes an important reduction of strength because the apparent cohesion at the toe reduces quickly and significantly.

Ultimately, this simple approach demonstrated that the hydrodynamic effects related to the overflow are important triggering factors for head-cut formation, but at the same time the loss of strength induced by the infiltration cannot be neglected. At the toe of the embankment, the initial unsaturated hydraulic conductivity is relatively high compared to the upper part of the downstream slope and the loss of suction is faster. The 'unsaturated' effects also explain why the breach formation in fine-grained embankment starts from the toe. Further and more rigorous analyses may help to understand the relative importance of these two effects.

6 REFERENCES

Al-Riffai, M., Nistor, I. 2010. Impact and analysis of geotechnical processes on earthfill dam breaching, *Natural Hazards* **55(1)**, 15-27.

Hanson, G. J., Cook, K. R., Hunt, S. L. 2005. Physical modeling of overtopping erosion and breach formation of cohesive embankments. *Transactions of the ASAE 2005*, **48(5)**, 1783–1794.

Morris, M. (2009a). *Breach initiation and growth: physical processes analysus of impact project breach field tests. FLOODsite Project Report , T06-08-11*.

Morris, M. (2009b). *Breaching Processes: A state of the art review*. *FLOODsite Project Report , T06-06-03*.

Pickert, G., Weitbrecht, V., and Bieberstein, A. 2011. Breaching of overtopped river embankments controlled by apparent cohesion. *Journal of Hydraulic Research*, **49(2)**, 143–156.

Tarantino, A., El Mountassir, G. 2013. Making unsaturated soil mechanics accessible for engineers: Preliminary hydraulic-mechanical characterisation and stability assessment. *Engineering Geology*, **165**, 89–104.

Volz, C. (2013). Numerical Simulation of Embankment Breaching Due to Overtopping. *VAW-Mitteilung*, **222(21371)**.

Walder, J. S., R. M. Iverson, J. W. Godt, M. Logan, and S. A. S. 2015. Overtopping of Noncohesive Earthen Dams. *Water Resources Research*, **51,** 6701–6724.

Wu, W. (2011). Earthen Embankment Breaching. *Journal of Hydraulic Engineering-Asce*, **137(12)**, 1549–1564.